Radiation from a Dielectric Coated Conducting Circular Cylinder Buried in a Conducting Corner (TM Case)

Hassan A. Ragheb

Department of Electrical Engineering
King Fahd University of Petroleum and Minerals, Dhahran, Saudi Arabia
hragheb@kfupm.edu.sa

Abstract –The paper presented a new design of a corner reflector antenna, fed through a dielectric coated slotted cylinder. An exact solution to a two dimensional problem is developed using the modal expansion solution for TM case. Computer program was developed to evaluate the radiation pattern, aperture conductance, and antenna gain. This antenna structure finds many applications on ships and airplanes in which the antenna is buried at corners of horizontal and vertical conducting planes. The radiation from this antenna showed many new features, which could not be achieved by the conventional corner reflector antenna.

Index Terms – Corner reflector antenna and dielectric coated slot antenna.

I. INTRODUCTION

Corner reflector antenna has been extensively investigated by many authors. The feed is usually considered as line source or dipole antenna. Various methods were employed to obtain the radiation characteristics of this antenna. For instance, analytical analysis [1], numerical analysis [2], and analysis using the geometrical theory of diffraction [3] were presented. Meanwhile, axial and circumferential slots of circular conducting cylinders were also examined by many investigators and different methods. The geometrical optics along with the residual series was represented in [4]. Green's function developed formulation was also introduced in [5]. In addition, an analytical development based on Fourier integral representation was presented in [6] and [7]. The combined slotted cylinder with reflecting corner was introduced in [8], to study the radiation from a transverse slot on a cylindrically tipped wedge. The wedge walls were considered infinite and analytical solution was obtained using Green's function method. Also radiation from an axial slot on a conducting circular cylinder with reflector wings was investigated in [9]. Integral equation for both TE and TM cases were developed using Green's functions. The resulting integral equation was numerically solved using moment method. A new geometry for cylindrically dielectric coated slotted antenna imbedded in a ground plane was the subject of the investigation in [10]. The radiation characteristic of this geometry was studied and showed that the ground plane can improve the antenna characteristics. Recently Romo et. al. [11], introduced an optimum design for cylindrical corner reflector antenna. Their results showed enhanced directive gain in the UHF bandwidth.

In this paper the dielectric coated slotted cylinder is assumed to be buried in a perfectly conducting corner of angle θ. The electric and magnetic fields for the TM case are assumed in terms of modal expansion of Fourier Bessel functions of unknown coefficients. The unknown coefficients were calculated by enforcing the boundary conditions. The formulation results in matrix equation of infinite dimensions, which can be truncated to a limited number of terms that satisfies the series convergence. A computer program was developed to calculate the antenna radiation pattern, aperture conductance, and antenna gain.

II. ANALYTICAL DEVELOPMENT (TM CASE)

A cross-sectional area of a conducting slotted circular cylinder of radius a coated with a

Submitted On: June 10, 2012
Accepted On: Nov. 23, 2012

concentric dielectric of outer radius *b*, permittivity ε, and permeability μ is illustrated in Fig. 1. The coated slotted cylinder is buried in a perfectly conducting corner as shown. The conducting corner planes are assumed to be infinitely long at $\phi = \theta^0/2$ and $\phi = -\theta^0/2$. The axial slot is centered at $\phi = \phi_0$ and has an angular angle equals to 2α. The space surrounding the conducting slotted cylinder is divided into two regions, region I ($a < \rho < b$) inside the dielectric coating, while region II ($\rho > b$, $-\theta^0/2 \geq \phi \geq \theta^0/2$) is outside the dielectric coated slotted cylinder in the space suspended by the corner conductors.

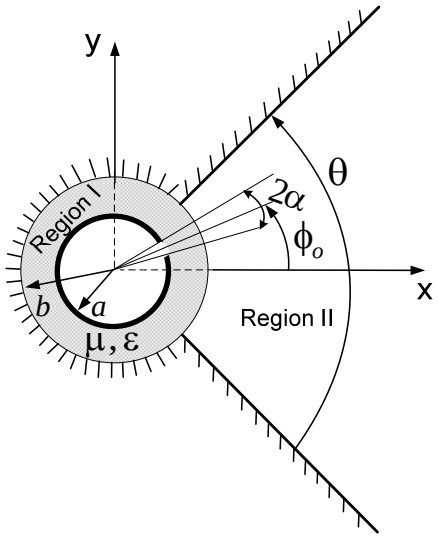

Fig. 1. Geometry of the problem.

The *z*-component of the electric field in region I can be written as,

$$E_z^{(I)} = E_o \sum_{n=-\infty}^{\infty} \left\{ A_n^{TM} J_n(k\rho) + B_n^{TM} N_n(k\rho) \right\} e^{jn\phi}. \quad (1)$$

The time dependence is assumed as $e^{j\omega t}$ and omitted throughout. The wave number $k_0 = 2\pi/\lambda$ where λ is the wavelength. Also, $J_n(x)$ and $N_n(x)$ are Bessel functions of the first and second kind, respectively of order *n* and argument *x*. Equation (1) is a solution of Helmholtz wave equation in cylindrical coordinates in region I, where A_n^{TM} and B_n^{TM} are unknown coefficients, which can be calculated from the boundary conditions. In a similar way one can write the *z*-component in region II as,

$$E_z^{(II)} = E_o \sum_{n=0}^{\infty} C_n^{TM} H_\nu^{(2)}(k_o\rho) \cos\nu\phi \qquad \nu = \frac{(2n+1)\pi}{\theta}. \quad (2)$$

Here $H_n^{(2)}(x)$ is the Hankel function of second kind with order *n* and argument *x*. C_n^{TM} are unknown coefficients that can be calculated from the boundary conditions. Furthermore, the boundary condition of vanishing $E_z^{(II)}$ at $\phi = \theta^0/2$ and $\phi = -\theta^0/2$ are satisfied in equation (2). The application of the boundary condition of vanishing $E_z^{(I)}$ on the surface of the conducting axially slotted cylinder results in,

$$E_o \sum_{n=-\infty}^{\infty} \left\{ A_n^{TM} J_n(ka) + B_n^{TM} N_n(ka) \right\} e^{jn\phi} = \begin{cases} E_z(\phi) & \phi_o - \alpha \leq \phi \leq \phi_o + \alpha \\ 0 & otherwise \end{cases}. \quad (3)$$

The *z*-component of the electric field on the axial slot aperture can be assumed as,

$$E_z(\phi) = E_o \cos\left(\frac{\pi(\phi - \phi_o)}{2\alpha} \right). \quad (4)$$

If one multiply both sides of equation (3) by $e^{-jm\phi}$ and integrates over ϕ from 0 to 2π, with some mathematical manipulations obtains,

$$B_m^{TM} = \frac{1}{N_m(ka)} \left\{ X_m^{TM} e^{-jm\phi_o} - A_m^{TM} J_m(ka) \right\} \quad (5)$$

where

$$X_m^{TM} = \frac{2\alpha \cos m\alpha}{\pi^2 - 4\alpha^2 m^2}.$$

The boundary condition at $\rho = b$ is given as,

$$E_z^{(I)} = \begin{cases} E_z^{(II)} & -\frac{\theta^o}{2} \leq \phi \leq \frac{\theta^o}{2} \\ 0 \quad otherwise \end{cases}. \quad (6)$$

Applying the above boundary condition, one can get,

$$\sum_{n=-\infty}^{\infty} \frac{X_n^{TM} N_n(kb) e^{-jn\phi_o}}{N_n(ka)} e^{jn\phi} + \sum_{n=-\infty}^{\infty} \frac{A_n^{TM} Y_n^{TM}}{N_n(ka)} e^{jn\phi} = \begin{cases} \sum_{n=0}^{\infty} C_n^{TM} H_\nu^{(2)}(k_o b) \cos\nu\phi & -\frac{\theta^o}{2} \leq \phi \leq \frac{\theta^o}{2} \\ 0 & otherwise \end{cases} \quad (7)$$

where

$$Y_n^{TM} = J_n(kb) N_n(ka) - J_n(ka) N_n(kb). \quad (8)$$

Multiplying both sides of equation (7) by $e^{-jm\phi}$ where (m = …, -3, -2, -1, 0, 1, 2, 3, …), and integrating over ϕ from 0 to 2π, we obtain,

$$2\pi\frac{X_m^{TM}N_m(kb)e^{-jm\phi_o}}{N_m(ka)}+2\pi\frac{A_m^{TM}Y_m^{TM}}{N_m(ka)}$$
$$=\sum_{n=0}^{\infty}C_n^{TM}H_\nu^{(2)}(k_ob)\;\;I_{mn}\;. \tag{9}$$

It can be re-arranged as,

$$A_m^{TM}=-\frac{X_m^{TM}N_m(kb)e^{-jm\phi_o}}{Y_m^{TM}}$$
$$+\frac{N_m(ka)}{2\pi Y_m^{TM}}\sum_{n=0}^{\infty}C_n^{TM}H_\nu^{(2)}(k_ob)\;\;I_{mn}\,. \tag{10}$$

where

$$I_{mn}=\begin{cases}\nu\left[\dfrac{2(-1)^{n+1}\cos\left(\frac{m\theta}{2}\right)}{m^2-\nu^2}\right] & \nu\neq m\\ \dfrac{\sin m\theta}{2m}+\dfrac{\theta}{2} & \nu=m\end{cases} \tag{11}$$

where n = 0, 1, 2, 3, … and m = …,-3, -2, -1, 0, 1, 2, 3, …. The magnetic fields in regions I and II can then be obtained from $H_\phi=(1/j\omega\mu)(dE_z/dr)$ as,

$$H_\phi^{(I)}=\frac{E_ok}{j\omega\mu}\sum_{n=-\infty}^{\infty}\frac{X_n^{TM}N_n'(k\rho)e^{-jn\phi_o}}{N_n(ka)}\;\;e^{jn\phi}$$
$$+\frac{E_ok}{j\omega\mu}\sum_{n=-\infty}^{\infty}\frac{A_n^{TM}}{N_n(ka)}\times$$
$$\left\{J_n'(k\rho)N_n(ka)-J_n(ka)N_n'(k\rho)\right\}e^{jn\phi} \tag{12}$$

and

$$H_\phi^{(II)}=\frac{E_ok_o}{j\omega\mu}\sum_{n=0}^{\infty}C_n^{TM}H_\nu^{(2)'}(k_o\rho)\cos\nu\phi\;. \tag{13}$$

The boundary condition of the continuous magnetic field H_ϕ at $\rho=b$ and $-\theta^0/2<\phi<\theta^0/2$ results in,

$$\sum_{n=-\infty}^{\infty}\frac{X_n^{TM}N_n'(kb)e^{-jn\phi_o}}{N_n(ka)}e^{jn\phi}+\sum_{n=-\infty}^{\infty}\frac{A_n^{TM}Y_n'^{TM}}{N_n(ka)}e^{jn\phi}$$
$$=\frac{1}{\sqrt{\varepsilon_r}}\sum_{n=0}^{\infty}C_n^{TM}H_\nu^{(2)'}(k_ob)\cos\nu\phi \tag{14}$$

where

$$Y_n'^{TM}=J_n'(kb)N_n(ka)-J_n(ka)N_n'(kb)\;. \tag{15}$$

Expanding equation (14) as,

$$\sum_{n=0}^{\infty}\frac{X_n^{TM}N_n'(kb)e^{-jn\phi_o}}{N_n(ka)}\;\;e^{jn\phi}$$
$$+\sum_{n=1}^{\infty}\frac{X_n^{TM}N_n'(kb)e^{jn\phi_o}}{N_n(ka)}\;\;e^{-jn\phi}$$
$$+\sum_{n=0}^{\infty}\frac{A_n^{TM}Y_n'^{TM}}{N_n(ka)}e^{jn\phi}$$
$$+\sum_{n=1}^{\infty}(-1)^n\frac{A_{-n}^{TM}Y_n'^{TM}}{N_n(ka)}e^{-jn\phi} \tag{16}$$
$$=\frac{1}{\sqrt{\varepsilon_r}}\sum_{n=0}^{\infty}C_n^{TM}H_\nu^{(2)'}(k_ob)\;\cos\nu\phi\,.$$

Since

$$I_{np}=I_{-np}\quad\text{and}\quad\nu=\frac{(2p+1)\pi}{\theta}\,. \tag{17}$$

Then, one can obtain,

$$(-1)^nA_{-n}^{TM}=-\frac{X_n^{TM}N_n(kb)e^{jn\phi_o}}{Y_n^{TM}}$$
$$+\frac{N_n(ka)}{2\pi Y_n^{TM}}\sum_{p=0}^{\infty}C_p^{TM}H_\nu^{(2)}(k_ob)\;\;I_{np} \tag{18}$$

Substituting from equations (10) and (18) into equation (16), one obtains,

$$\sum_{n=0}^{\infty}\left(\frac{X_n^{TM}N_n'(kb)e^{-jn\phi_o}}{N_n(ka)}\right.$$
$$\left.-\frac{X_n^{TM}N_n(kb)e^{-jn\phi_o}}{Y_n^{TM}}\frac{Y_n'^{TM}}{N_n(ka)}\right)e^{jn\phi}$$
$$+\sum_{n=1}^{\infty}\left(\frac{X_n^{TM}N_n'(kb)e^{jn\phi_o}}{N_n(ka)}\right.$$
$$\left.-\frac{X_n^{TM}N_n(kb)e^{jn\phi_o}}{Y_n^{TM}}\frac{Y_n'^{TM}}{N_n(ka)}\right)e^{-jn\phi} \tag{19}$$
$$+\sum_{n=0}^{\infty}\left(\frac{Y_n'^{TM}}{2\pi Y_n^{TM}}\sum_{p=0}^{\infty}C_p^{TM}H_\nu^{(2)}(k_ob)\;\;I_{np}\right)$$
$$(e^{jn\phi}+e^{-jn\phi})$$
$$=\frac{1}{\sqrt{\varepsilon_r}}\sum_{p=0}^{\infty}C_p^{TM}H_\nu^{(2)'}(k_ob)\;\;\cos\nu\phi\;.$$

Equation (19) can be simplified as,

$$\sum_{n=0}^{\infty}\frac{2\varepsilon_n X_n^{TM}}{\pi kbY_n^{TM}}\cos n(\phi-\phi_o) + \sum_{n=0}^{\infty}\varepsilon_n\left(\frac{Y_n'^{TM}}{2\pi Y_n^{TM}} \sum_{p=1}^{\infty}C_p^{TM}H_\nu^{(2)}(k_o b)\;\; I_{np}\right)\cos n\phi = \frac{1}{\sqrt{\varepsilon_r}}\sum_{p=0}^{\infty}C_p^{TM}H_\nu^{(2)'}(k_o b)\;\cos\nu\phi\,. \tag{20}$$

Multiplying both sides of equation (20) by cos $m\phi$ (m = 0, 1, 2, 3, …), and integrating over ϕ from $-\theta^0/2$ to $\theta^0/2$ to obtain,

$$\sum_{n=0}^{\infty}\frac{2\varepsilon_n X_n^{TM}}{\pi kbY_n^{TM}}\cos n\phi_o\;\; K_{mn} + \sum_{n=0}^{\infty}\varepsilon_n\left(\frac{Y_n'^{TM}}{2\pi Y_n^{TM}} \sum_{p=1}^{\infty}C_p^{TM}H_\nu^{(2)}(k_o b)\;\; I_{np}\right)K_{mn} = \frac{1}{\sqrt{\varepsilon_r}}\sum_{p=0}^{\infty}C_p^{TM}H_\nu^{(2)'}(k_o b)\;\; K_{m\nu} \tag{21}$$

$$K_{mn}=\begin{cases}\dfrac{\sin(m+n)\frac{\theta}{2}}{(m+n)}+\dfrac{\sin(m-n)\frac{\theta}{2}}{(m-n)} & n\neq m\\ \dfrac{\sin m\theta}{2m}+\dfrac{\theta}{2} & n=m,\end{cases} \tag{22}$$

where n= 0, 1, 2,… and m = 0, 1, 2,… Rearranging equation (21) takes the form,

$$\sum_{p=0}^{\infty}C_p^{TM}\left\{\frac{1}{\sqrt{\varepsilon_r}}H_\nu^{(2)'}(k_o b)\;\; K_{m\nu} - H_\nu^{(2)}(k_o b)\sum_{n=0}^{\infty}\frac{\varepsilon_n Y_n'^{TM}}{2\pi Y_n^{TM}}I_{np}K_{mn}\right\} = \sum_{n=0}^{\infty}\frac{2\varepsilon_n X_n^{TM}}{\pi kbY_n^{TM}}\cos n\phi_o K_{mn} \tag{23}$$

where ε_n is 1 for n = 0 and 2 otherwise. Equations (23) can be written in a matrix form,

$$[Z][C^{TM}]=[M] \tag{24}$$

where

$$Z_{mp}=\frac{1}{\sqrt{\varepsilon_r}}H_\nu^{(2)'}(k_o b)\;\; K_{m\nu} - H_\nu^{(2)}(k_o b)\sum_{n=0}^{\infty}\frac{\varepsilon_n Y_n'^{TM}}{2\pi Y_n^{TM}}I_{np}K_{mn}\,,$$

$$M_m=\sum_{n=0}^{\infty}\frac{2\varepsilon_n X_n^{TM}}{\pi kbY_n^{TM}}\cos n\phi_o K_{mn}\,.$$

III. RADIATION PATTERN AND SLOT CONDUCTANCE

The far zone radiation pattern for the electric field of the TM case can be calculated using the asymptotic expression of the Hankel function, i.e.,

$$E_z^{(II)}=E_o\sum_{n=1}^{\infty}C_n^{TM}H_\nu^{(2)}(k_o\rho)\sin\nu\phi\quad,\nu=\frac{n\pi}{\theta}$$

$$E_z^{(I)}=\sqrt{\frac{2}{\pi kr}}\quad e^{-jkr}\;\; e^{j\pi/4}\quad P_{TM}(\phi)$$

where

$$P_{TM}(\phi)=\sum_{n=0}^{\infty}j^{\frac{(2n+1)\pi}{\theta}}C_n^{TM}\cos\frac{(2n+1)\pi}{\theta}\phi. \tag{25}$$

The antenna gain and the aperture conductance are quantities of interest. Following the definition of Richmond [10], one can obtain the antenna gain as,

$$G(\phi)=\frac{2\,|\,P_{TM}(\phi)\,|^2}{\sum_{n=0}^{\infty}|\,C_n^{TM}\;|^2} \tag{26}$$

and the aperture conductance is

$$G_a/\lambda=\frac{1}{120\pi^2}\frac{\sum_{n=1}^{\infty}|\,C_n^{TM}\;|^2}{|\,E_o\,|^2}\,. \tag{27}$$

IV. RESULTS AND DISCUSSION

The accuracy of our computations will be verified first through two different methods. In the first, the integral equation formulation along with the moment method is employed to solve the problem when ε_r = 1. Figure 2, illustrates the far field pattern due to IEF and the present method. An excellent agreement is found in the range of -39^o to 39^o while the discrepancy in the rest is due to the finite size of the corner reflector considered in IEF (MoM). The second verification is through

some special cases published in [12]. The example shown in Fig. 3, illustrates the far field radiation pattern of a dielectric coated slotted cylinder embedded in a conducting ground plane. In this case the corner angle is considered as $\theta = 180^{o}$. The far field pattern obtained using the current formulation is compared with the corresponding published pattern [12] obtained for the same example. An excellent agreement is found. The parameters of both examples are given in the figure caption.

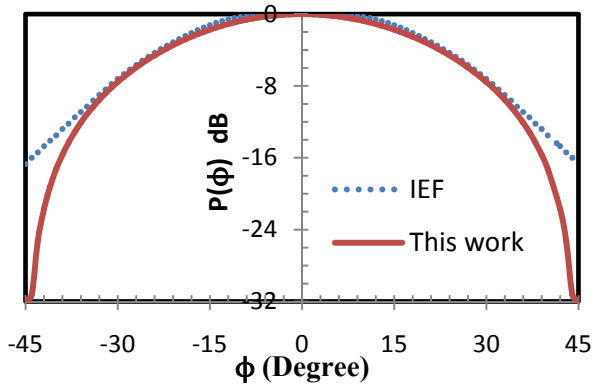

Fig. 2. Far field pattern of an axial slot on a dielectric coated conducting circular cylinder embedded in ground plane ($\theta = 90^0$, $a = 0.4\ \lambda$, $b = 0.69\ \lambda$, $2\alpha = 10^0$, $\phi_0 = 0^0$, $\varepsilon_r = 1$, and $\mu_r = 1$).

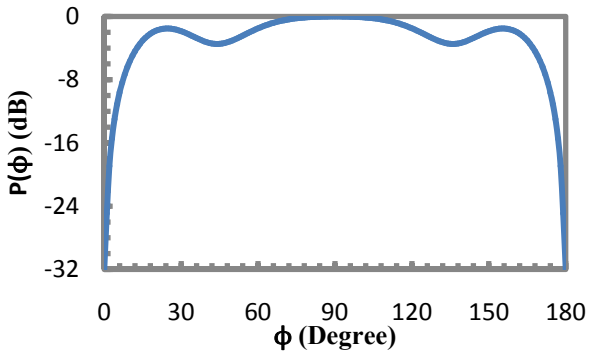

Fig. 3. Far field pattern of an axial slot on a dielectric coated conducting circular cylinder embedded in ground plane (($\theta = 180^0$, $a = 0.51\ \lambda$, $b = 0.63\ \lambda$, $2\alpha = 10^0$, $\phi_0 = 90^0$, $\varepsilon_r = 3.1$, and $\mu_r = 1$)

Figure 4, shows the antenna gain versus the dielectric thickness. The results obtained from the present formulation are compared with the corresponding results in [12], where an excellent agreement is noticed. Aperture conductance is also compared with same example presented in [12]. Our results showed in Fig. 5 are in typical agreement with the corresponding ones in [12].

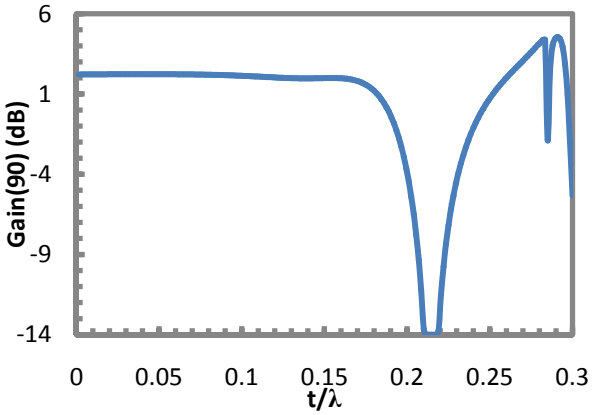

Fig. 4. Gain at 90^0 of an axial slot on a dielectric coated conducting circular cylinder embedded in ground plane ($\theta = 180^0$, $a = 0.51\ \lambda$, $b = 0.63\ \lambda$, $2\alpha = 10^0$, $\phi_0 = 90^0$, $\varepsilon_r = 3.1$, and $\mu_r = 1$).

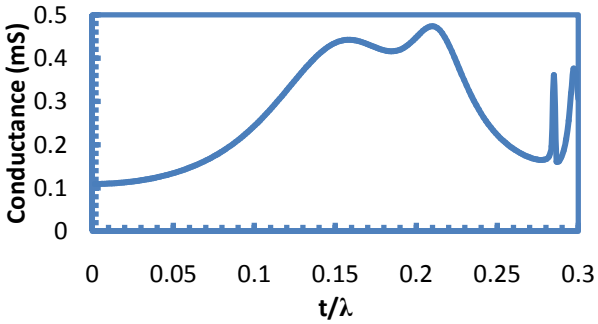

Fig. 5. Aperture conductance of an axial slot on a dielectric coated conducting circular cylinder embedded in ground plane ($\theta = 180^0$, $a = 0.51\ \lambda$, $b = 0.63\ \lambda$, $2\alpha = 10^0$, $\phi_0 = 90^0$, $\varepsilon_r = 3.1$, and $\mu_r = 1$).

In the following examples the corner reflector angle is considered as $\theta = 90^0$. In Fig. 6, the far field pattern corresponding to different values of dielectric coating are presented. As can be seen from Fig. 6, as the coating radius increases, the main beam gets narrower and side lobes starts to appear.

Another case is also presented in Fig. 7 for the far field patterns due to different dielectric thicknesses. A similar behavior is noticed in which the main beam gets narrower as the dielectric thickness increases. Increasing the dielectric thickness more creates side lobes.

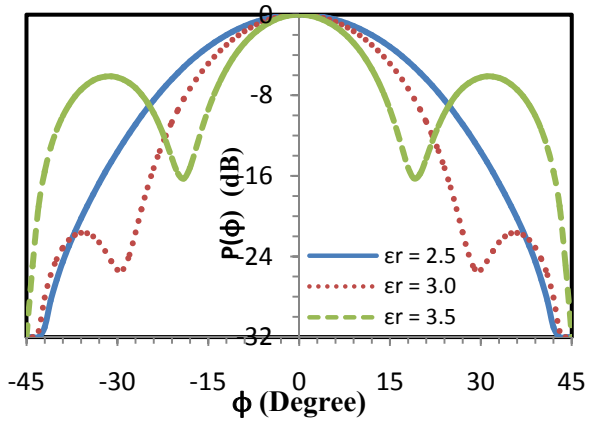

Fig. 6. Far field pattern of an axial slot on a dielectric coated conducting circular cylinder embedded in conducting corner ($\theta = 90^0$, a = 0.51 λ, b = 0.72 λ, $2\alpha = 10^0$, $\phi_0 = 0^0$, and $\mu_r = 1$).

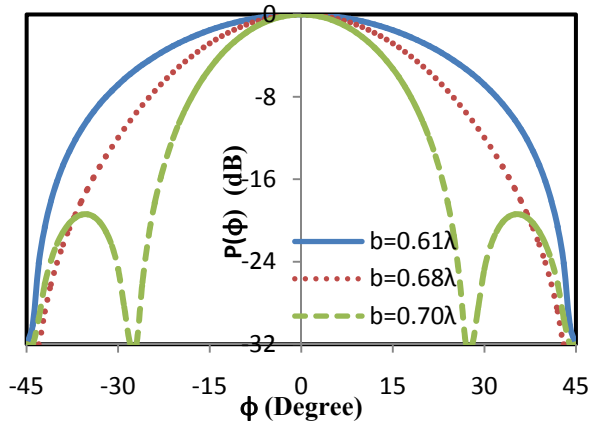

Fig. 7. Far field pattern of an axial slot on a dielectric coated conducting circular cylinder embedded in conducting corner ($\theta = 90^0$, a = 0.51 λ, $2\alpha = 10^0$, $\varepsilon_r = 3.6$, $\phi_0 = 0^0$, and $\mu_r = 1$).

The antenna gain at $\phi = 45^0$ versus the dielectric coating thickness for different dielectric permittivity is illustrated in Fig. 8. As one can see from Fig. 8, the gain at 45^0 angle, decreases as the dielectric permittivity increases. In addition, the higher the dielectric permittivity, the lower is the dielectric thickness before the gain drops.

Finally the aperture conductance at different dielectric permittivity versus dielectric thickness is shown in Fig. 9. It is noticed that the peak of the conductance occurs at lower thickness as the dielectric permittivity increases.

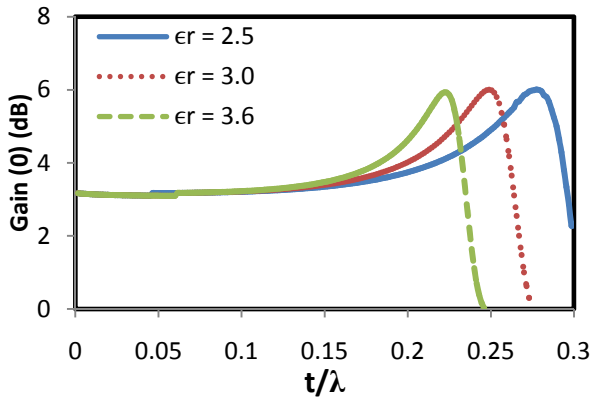

Fig. 8. Gain at 0^0 of an axial slot on a dielectric coated conducting circular cylinder embedded in conducting corner ($\theta = 90^0$, a = 0.45 λ, $2\alpha = 10^0$, $\phi_0 = 0^0$, and $\mu_r = 1$).

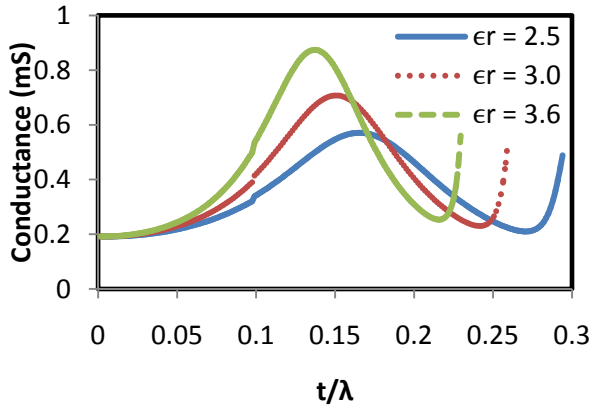

Fig. 9. Aperture conductance of an axial slot on a dielectric coated conducting circular cylinder embedded in conducting corner ($\theta = 90^0$, a = 0.45 λ, $2\alpha = 10^0$, $\phi_0 = 0^0$, and $\mu_r = 1$).

V. CONCLUSUON

New design of a corner reflector antenna, fed through a dielectric coated slotted cylinder was analyzed. The radiation pattern, aperture conductance and antenna gain was calculated. The study showed that for a constant gain at the bi-sector angle, the dielectric thickness decreases as the dielectric permittivity increases. Also the maximum conductance occurs at lower dielectric thickness as permittivity increases.

REFERENCES

[1] J. R. Wait, "On the theory of an antenna with an infinite corner reflector," *Canadian Journal of Physics*, vol. 32, pp. 365, 1954.

[2] A. C. Willson and H. V. Cottony, "Radiation pattern of finite size corner reflector antenna," *IRE Trans. Antennas and Propag.*, vol. 8, pp. 144-148, 1960.

[3] H. A. Ragheb, A. Z. Elsherbeni, and M. Hamid, "Radiation characteristics of the corner array," *Int. Journal of Electronics*, vol. 60, pp. 229-238, 1986.

[4] S. Sensiper, "Cylindrical radio waves," *IRE Trans. Antennas and Propag.*, vol. 5, pp. 56-70, 1957.

[5] C. H. Papas, "Radiation from a transverse slot in an infinite cylinder," *J. of Mathematics and Phys.*, vol. XXVII, pp. 227-236, 1949.

[6] S. Silver and W. K. Saunders, "The radiation from transverse rectangular slot in a circular cylinder," *J. of Appl. Phys.*, vol. 21, pp. 153-158, Feb. 1950.

[7] L. L. Bailin, "Radiation field produced by a slot in a large circular cylinder," *IRE Trans. Antennas and Propag.*, vol. 3, pp. 128-137, 1955.

[8] J. Wait and S. Kahana, "Radiation from a slot in a cylindrically tipped wedge," *Canadian Journal of Phys.*, vol. 32, pp. 714-721, 1954.

[9] H. Ragheb, A. Sebak, and L. Shafai, "Radiation from an axial slot on a conducting circular cylinder with reflector wings," *J. of Electromagnetic Waves and Appl.*, vol. 11, pp. 65-76, 1997.

[10] J. Richmond, "Axial slot antenna on dielectric-coated elliptic cylinder," *IEEE Trans. Antennas and Propag.*, vol. 37, pp. 1235-1241, Oct. 1989.

[11] J. A. Romo, I. F. Anitzine, and J. Garate, "Optimized design of cylindrical corner reflectors for applications on TV broadband antennas," *Applied Computational Electromagnetics Society (ACES) Journal*, vol. 26, no. 11, pp. 937-944, Nov. 2011.

[12] H. A. Ragheb and U. M. Johar, "Radiation characteristics of an infinite dielectric-coated axially slotted cylindrical antenna partly embedded in a ground plane," *IEEE Trans. Antennas and Propag.*, vol. 46, no. 10, pp. 1542-1547, Oct. 1998.

Hassan Ragheb was born in Port-Said, Egypt, in 1953. He received the B.Sc. degree in Electrical Engineering from Cairo University, Egypt in 1977 and the M.Sc. and Ph.D. degrees in Electrical Engineering from the University of Manitoba, Winnipeg, Canada in 1984 and 1987, respectively. From 1987 to 1989, he was a research assistant in the Department of Electrical Engineering, University of Manitoba. In 1989, he joined the Department of Electrical Engineering at the King Fahd University of Petroleum and Minerals, where he is now a Professor of Electrical Engineering. His research interests include electromagnetic scattering by multiple and coated objects, micro strip antennas, phased arrays, slot and open ended waveguide antennas.